Tableau 3. *Distances interatomiques et angles*

Les distances As_iO_j sont soulignées en Å. Les angles $O_jAs_iO_k$ sont en dessus de la diagonale en degrés et 1/100°. En dessous de la diagonale sont données les distances O–O en Å dans le même tétraèdre.

(*a*) Les tétraèdres AsO_4

As(1)	O(1)	O(2)	O(3)	O(4)
O(1)	1,654 (3)	100,8 (2)	113,8 (2)	118,6 (2)
O(2)	2,606 (5)	1,727 (4)	102,4 (2)	111,3 (2)
O(3)	2,843 (5)	2,701 (6)	1,740 (5)	108,6 (2)
O(4)	2,848 (5)	2,667 (4)	2,761 (7)	1,659 (5)
As(2)	O(5)	O(6)	O(7)	O(8)
O(5)	1,686 (4)	113,9 (2)	102,0 (2)	108,8 (2)
O(6)	2,799 (5)	1,652 (4)	108,8 (2)	114,8 (2)
O(7)	2,667 (7)	2,765 (6)	1,746 (5)	107,5 (2)
O(8)	2,739 (5)	2,810 (5)	2,765 (5)	1,682 (3)

(*b*) Environnement du strontium et distances Sr–O

Sr–O(1)^{I}	2,612 (3)	Sr–O(5′)^{II}	2,567 (5)
Sr–O(1′)	2,547 (3)	Sr–O(6)^{III}	2,600 (4)
Sr–O(2)^{I}	2,772 (3)	Sr–O(6′)^{IV}	2,559 (3)
Sr–O(4)	2,511 (4)	Sr–O(7)	2,826 (4)

(*c*) Distances les plus courtes O–O dans les sites tétraédriques différents

O(2)–O(4′)^{V}	2,666 (4)	O(7)–O(3′)^{V}	2,862 (6)
O(3)–O(8′)^{VI}	2,700 (5)	O(8)–O(8′)^{VII}	2,474 (8)
O(5)–O(5′)^{II}	2,435 (8)		

(*d*) Les notations utilisées

Les chiffres arabes de 1 à 8 correspondent à des numéros d'atomes indépendants cristallographiquement.
Le sigle prime indique la position $\bar{x},\bar{y},\bar{z}$.
Les chiffres romains correspondent aux positions suivantes: (I) $x, y, 1+z$; (II) $\bar{x}, 1-y, 1-z$; (III) $x, -1+y, z$; (IV) $\bar{x}, 1-y, \bar{z}$; (V) $1-x, 1-y, \bar{z}$; (VI) $1-x, 1-y, 1-z$; (VII) $1-x, 2-y, 1-z$.

fait, nous devons avoir trois atomes d'hydrogène en position générale et deux autres en position spéciale en $\frac{1}{2},0,\frac{1}{2}$ et $0,\frac{1}{2},\frac{1}{2}$. Nous donnons les plus courtes distances O–O dans des sites tétraédriques différents, qui vérifient cette hypothèse. Toutes les distances interatomiques et angles de liaison figurent dans le Tableau 3. Il nous a été impossible de localiser avec précision les protons, du fait que les séries de Fourier-différence à ce niveau se sont révélées infructueuses. Il serait donc intéressant de faire une étude par diffraction neutronique afin de déterminer la position des atomes d'hydrogène. Notons pour terminer que cette structure a de très grandes analogies avec celle étudiée par Ferraris, Jones & Yerkess (1972).

Afin de faciliter cette comparaison, nous avons adopté les mêmes notations pour les atomes. En effet, si nous comparons les deux structures $Sr(H_2AsO_4)_2$ et $Ca(H_2AsO_4)_2$ qui ont des paramètres cristallins assez voisins, nous remarquons surtout un très net déplacement de l'ensemble des atomes selon l'axe *c*.

Références

FERRARIS, G., JONES, D. W. & YERKESS, J. (1972). *Acta Cryst.* B**28**, 2430–2437.

GUÉRIN, H. & MICHEL, S. (1942). *C. R. Acad. Sci.* **214**, 1004–1005.

PREWITT, C. T. (1966). *SFLS*-5. Report ORNL-TM-305. Oak Ridge National Laboratory, Tennessee.

TARTAR, H. V. & RICE, M. R. (1931). *J. Am. Chem. Soc.* **53**, 3949.

Acta Cryst. (1979). B**35**, 1052–1059

The Nature of the Chemical Bonding in Boron Carbide, $B_{13}C_2$. I. Structure Refinement

BY A. KIRFEL, A. GUPTA AND G. WILL

Mineralogisches Institut der Universität Bonn, Lehrstuhl für Mineralogie und Kristallographie, Poppelsdorfer Schloss, 5300 Bonn, Federal Republic of Germany

(*Received* 30 *December* 1978; *accepted* 6 *February* 1979)

Abstract

The crystal structure of synthetic $B_{13}C_2$ has been investigated by X-ray diffraction. Atomic parameters were determined from both conventional refinement techniques, with the spherical-atom model, and multipole expansion refinement. The analysis of the results shows the scale factor and some of the vibrational parameters to be considerably biased by bonding effects. Bias could be reduced by high-order refinements leading to parameters which agree with the results of the multipole expansion refinement within the

0567-7408/79/051052-08$01.00

limits of error. The investigation of the charge character of the atoms does not yield significant indication of a deviation of the B_{12} icosahedron from electric neutrality.

Introduction

Boron carbide has been a controversial compound for many years and has attracted much interest from crystallographers and theoretical chemists. The composition of boron carbide in its ideal form is $B_{13}C_2 = (B_{12})CBC$. It is the only stoichiometric compound in the rhombohedral phase of the B/C system observed so far (Matkovich & Economy, 1977). The crystal structure is based on a cubic closest-packing of B_{12} icosahedra. The inter-icosahedral openings are occupied by two C and a B atom in a linear C–B–C arrangement (Fig. 1). Thus, there are two structural units, the C–B–C chain and the B_{12} icosahedron, and the interest concentrates on the bonding features in the units themselves and between them. In the B_{12} unit each B atom has five nearest neighbors in the icosahedron, apart from the external atom, to which it is bonded. This configuration makes the interpretation of the bonding in terms of ordinary rules of covalency impossible.

Longuet-Higgins & Roberts (1955) investigated the electronic structure of the icosahedral B_{12} unit by molecular orbital calculations. It was found that thirteen bonding orbitals are available for holding the icosahedron together, besides the twelve outward-pointing equivalent orbitals of the separate atoms. Thus each icosahedron, providing 36 valence electrons, requires 38 electrons for a closed-shell type structure, and the missing two electrons have to be attracted from elsewhere. The concept led to the correct prediction of the $B_{12}H_{12}^{2-}$ ion and was employed to explain the stability of $B_4C=(B_{12})CCC$. However, $B_{13}C_2$ is one electron deficient and possesses an even higher melting point than B_4C. Thus, there is great interest in obtaining experimental evidence about the assumed charge transfer from the chain towards the icosahedron. Results about a charge redistribution in $B_{13}C_2$ were first obtained by Will & Kossobutzki (1976*a*,*b*). The data set, however, was limited and not suitable for electron density studies. New X-ray diffraction measurements on a $B_{13}C_2$ crystal for the determination of the electron density and analysis of the valence electron distribution seemed therefore desirable.

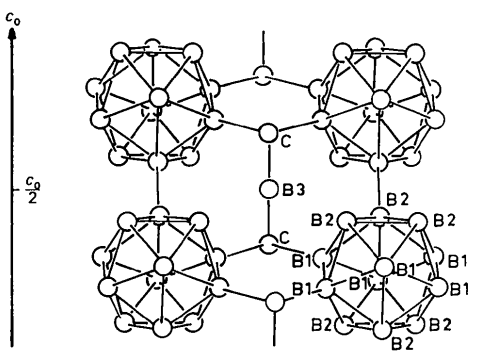

Fig. 1. The structure of $B_{13}C_2$.

In the first part of our work we report an X-ray diffraction study on a $B_{13}C_2$ crystal of well-defined composition and the analysis of the reflection data by least-squares calculations, with the conventional spherical-atom model as well as a model allowing deviations from spherical symmetry by simultaneous refinement of atomic multipole functions. It is the aim of this paper to establish a scale factor and atomic parameters which are least biased by bonding effects, as a basis for subsequent electron density studies by Fourier methods. Additionally, the question of charge transfer in and from the chain on the one hand, and in the B_{12} icosahedron on the other, is investigated in first-order approximation. This may serve as a test for the Longuet-Higgins & Roberts (1955) theory of B_{12} icosahedra in condensed boron systems.

Experimental

The boron carbide single crystals for the present study were obtained from Professor Amberger, Munich. They were synthesized by pyrolytic methods on a carbon–boron–nitride plate at approximately 1273 K (Amberger, Druminski & Ploog, 1971). A boron carbide crystal with idiomorphic faces and 0·2 × 0·2 × 0·4 mm was selected for X-ray diffraction. Weissenberg photographs were used to check the quality of the crystal and the space group $R\bar{3}m$ (Will & Kossobutzki, 1976*a*).

The diffraction data were collected on an automatic four-circle diffractometer (Syntex $P2_1$) with Mo $K\alpha$ radiation (λ = 0·7107 Å) and a graphite monochromator ($2\theta_m$ = 12·2°). The unit-cell parameters were determined by least-squares calculations from the angular settings of 25 independent reflections. D_x = 2·452 Mg m^{-3}; the experimental density is D_e = 2·48 Mg m^{-3} (Amberger, 1977). According to Amberger, Druminski & Ploog (1971), D_x and D_e correspond to carbon contents of 14·1 and 14·4 wt%, which are close to the theoretical 14·59 wt%. The intensity measurements were carried out in the θ–2θ scan mode with a 1·0° plus (α_1,α_2)-dispersion scan range. The scan speed was adjustable between 0·5 and 10·0° per min, and the total background counting time equalled the time spent for the peak count. Four standard reflections were remeasured after every 30 reflections. Up to a maximum 2θ = 100° (sin θ/λ = 1·078 Å^{-1}) the complete sphere was scanned, leading to 6000 recorded reflections (omitting standards).

Table 1. *Crystallographic data*

Formula	$B_{13}C_2$
M_r	164·56
Space group	$R\bar{3}m$
a_{hex}	5·633 (1) Å
c_{hex}	12·164 (2)
a_{rhomb}	5·198 (2)
α_{rhomb}	65·62°
V_{hex}	334·3 (1) Å^3
Z_{hex}	3
D_x	2·452 Mg m^{-3}
μ(Mo $K\bar{\alpha}$)	0·0518 mm^{-1}

Table 2. *Intensity measurement and processing*

Radiation	Mo $K\alpha$ ($\lambda = 0·7107$ Å)
Monochromatization	Graphite crystal ($2\theta = 12·2°$)
Crystal dimensions	0·2 × 0·2 × 0·4 mm
Maximum θ	50·0°
$(\sin\theta/\lambda)_{max}$	1·078 Å^{-1}
Scan mode	θ–2θ step scan
Scan angle	1·0°
Number of steps	96
Scan speed	0·5–10·0 ° min^{-1}
Number of monitor reflections	4
Monitor reflection interval	30
Number of reflections recorded	6000
Number of unique reflections	721
Number of unobserved reflections [$I < 1·5\,\sigma(I)$]	246
Internal match Rf	0·021

In the data reduction the intensities were adjusted to the fluctuations of the sum of the standards. Symmetry-related reflections were averaged, resulting in a set of 721 unique reflections, of which 246 were regarded as unobserved ($I < 1·5\sigma$). The internal agreement index of the data based on the deviations of the $|F_{h,i}|$ of equivalent reflections from their means $|\bar{F}_h|$ was

$$Rf = \sum_h \sum_i \big||\bar{F}_h| - |F_{h,i}|\big| / \sum_h \sum_i |F_{h,i}| = 0·021.$$

No absorption corrections were applied ($\mu = 0·0518$ mm^{-1}). The results of the crystal measurements and the data collection are summarized in Tables 1 and 2.*

Structure refinement

The structure refinement was carried out with *ORFLS* (Busing, Martin & Levy, 1962) and the multipole expansion program *LS-EXP* (Hirshfeld, 1971; Harel & Hirshfeld, 1975).

* Lists of structure factors and anisotropic thermal parameters have been deposited with the British Library Lending Division as Supplementary Publication No. SUP 34259 (5 pp.). Copies may be obtained through The Executive Secretary, International Union of Crystallography, 5 Abbey Square, Chester CH1 2HU, England.

(*a*) *Conventional refinement*

The atomic coordinates determined by Will & Kossobutzki (1976*a*,*b*) were used as starting parameters for full-matrix least-squares minimization of $\sum w[(1/K)|F_o| - |F_c|]^2$ with $w = 1/\sigma^2(F)$.

Atomic form factors for B and C were taken from *International Tables for X-ray Crystallography* (1974). Positional and anisotropic thermal parameters were refined for all atoms along with the overall scale factor K. The inclusion of an isotropic extinction coefficient g (Zachariasen, 1963) in the list of variables did not affect R. Hence correction for secondary extinction was considered unnecessary.

To reduce bias in the refined parameters from the aspherical valence-electron distribution, additional high-order refinements were carried out with only data with $\sin\theta/\lambda \geq 0·65$ Å^{-1} (HO1); $\sin\theta/\lambda \geq 0·75$ Å^{-1} (HO2) and $\sin\theta/\lambda \geq 0·85$ Å^{-1} (HO3). The necessity of doing so is reflected in the improved agreement index and goodness of fit figures (Table 3).

Since the multiplicities of the atoms scale the scattering factors in the least-squares calculations, they may serve to count the number of electrons effectively assigned to each site. Therefore, the occupancies of the B and C atoms were also varied in the final stages of the refinements. Since the occupancies usually are highly correlated with the scale factor, these variables were refined independently in subsequent cycles. No total charge constraint was imposed. The results of the various conventional refinements are compiled in Tables 3 to 7, which contain corresponding results, if any, of the second refinement procedure described below.

(*b*) *Multipole expansion refinement*

Refinement was by minimization of $\sum w(|F_o| - K|F_c|)^2$. In the program *LS-EXP* the charge density of a stationary atomic arrangement is expressed as a superposition of spherical free-atom densities ρ_j^{at}, defined by the input scattering curves, plus a deformation density $d\rho$, approximated by a linear combination of localized atomic deformation functions ψ_{jl},

$$\rho = \sum_j \left(\rho_j^{at} + \sum_l c_{jl}\psi_{jl}\right).$$

Thus each atom has to be assigned an orthogonal coordinate system and with respect to this a set of multipole functions, which must comply with the atomic site symmetry. The orientations of the coordinate systems are definable by specification of a first and second neighbor for the atom considered. Then the x axis points towards the first neighbor atom and the y axis is in the plane through the three atoms. Vibrational motion is treated by the convolution approximation, in which each atomic fragment is supposed to move as a rigid unit. The adjustment of all sets of

Table 3. *Agreement indices of least-squares refinements*

(Second row: conventional refinements including independent variation of occupancies.)

Refinement	LO	All data	HO1	HO2	HO3	Multipole expansion
sin θ/λ (Å^{-1})	0·0–0·65	0·0–1·08	0·65–1·08	0·75–1·08	0·85–1·08	0·0–1·08
Number of reflections	114	721	600	542	476	721
Number of variables		14	14	14	14	69
Number of variables including occupancies	18	18	18	18	18	
Scale factor		0·479 (2)	0·454 (2)	0·449 (3)	0·450 (4)	0·453 (1)
	0·484 (2)	0·480 (1)	0·454 (1)	0·449 (1)	0·449 (1)	
Overall R values						
R		0·080	0·096	0·117	0·140	0·077
	0·044	0·079	0·096	0·117	0·140	
R_w		0·050	0·031	0·038	0·041	0·028
	0·053	0·050	0·031	0·038	0·041	
R values omitting unobserved reflections						
R		0·047	0·042	0·048	0·055	0·044
	0·043	0·046	0·042	0·048	0·055	
R_w		0·052	0·026	0·030	0·032	0·028
	0·053	0·049	0·025	0·030	0·032	
Goodness of fit		2·10	0·82	0·79	0·80	1·20
	4·18	1·96	0·81	0·78	0·80	

Table 4. *Atomic fractional coordinates* ($\times 10^5$) *with e.s.d.'s in parentheses*

Atomic sites are (in the hexagonal description): B(1) and B(2) in 18(h): $x, -x, z$; B(3) in 3(b): 0,0,½; C in 6(c): 0,0,z.

Refinement			All data	HO1	HO2	HO3	Multipole expansion
B(1)	18(h)	x	16310 (17)	16311 (9)	16307 (11)	16306 (12)	16323 (13)
		z	64114 (6)	64116 (3)	64119 (4)	64116 (5)	64106 (4)
B(2)	18(h)	x	22555 (16)	22545 (9)	22547 (10)	22546 (13)	22539 (12)
		z	78008 (6)	78007 (3)	78006 (4)	78001 (5)	77980 (4)
C	6(c)	z	61747 (2)	61760 (7)	61767 (8)	61762 (9)	61824 (8)

Table 5. *Atomic vibrational parameters* u_{ij} ($\times 10^4$ Å^2) *with e.s.d.'s in parentheses*

Special relationships for all atoms:

$$u_{11} = u_{22},\ u_{12} = u_{11}/2,\ u_{13} = u_{23} = 0.$$

Refinement		All data	HO1	HO2	HO3	Multipole expansion
B(1)	u_{11}	47 (1)	41 (1)	40 (2)	39 (2)	38 (3)
	u_{33}	60 (3)	54 (2)	52 (2)	53 (2)	50 (3)
B(2)	u_{11}	51 (1)	45 (1)	43 (2)	44 (2)	44 (3)
	u_{33}	49 (7)	42 (2)	41 (2)	40 (2)	45 (3)
B(3)	u_{11}	105 (5)	100 (4)	97 (4)	97 (5)	102 (8)
	u_{33}	171 (6)	134 (4)	124 (5)	118 (6)	113 (6)
C	u_{11}	44 (2)	42 (2)	41 (2)	42 (2)	38 (4)
	u_{33}	135 (6)	126 (2)	118 (3)	115 (3)	117 (6)

deformation functions is by variation of the multipole coefficients c_{jl} added to the list of conventional crystallographic variables.

The deformation functions are of the general form:

$\psi_{jl} = N_n\, r^n \exp(-\alpha r_a) \cos^n \theta_K$,

r_a = distance from atomic center,

n = multipole order (0 to 4),

θ_K = angle between radius vector r and specified polar axis k,

α = constant describing radial breadth,

N_n = normalizing factor.

Table 6. *Selected bond distances* (Å) *with e.s.d.'s in parentheses*

Refinement	All data	HO1	HO2	HO3	Multipole expansion
Intra-icosahedral bonds					
B(1)–B(1^{i})	1·773 (1)	1·773 (1)	1·773 (1)	1·773 (1)	1·773 (1)
B(1)–B(2)	1·797 (1)	1·796 (1)	1·796 (1)	1·795 (1)	1·793 (2)
B(1)–B(2^{i})	1·806 (1)	1·806 (0)	1·807 (1)	1·806 (1)	1·803 (2)
B(2)–B(2^{ii})	1·821 (1)	1·823 (0)	1·823 (0)	1·823 (1)	1·824 (1)
Other bonds					
B(1)–C	1·617 (1)	1·617 (0)	1·617 (0)	1·616 (0)	1·617 (1)
B(2)–B(2^{iii})	1·732 (1)	1·731 (0)	1·731 (1)	1·732 (1)	1·735 (1)
B(3)–C	1·429 (0)	1·430 (0)	1·431 (1)	1·431 (1)	1·438 (3)

Equivalent positions:
(i) $\frac{1}{2}-x, \frac{1}{2}+y-x, \frac{1}{2}-z$
(ii) $\bar{y}, x-y, z$
(iii) $\frac{1}{2}-x, \frac{1}{2}-y, \frac{1}{2}-z$.

After completion of the refinement with all data, the final sets of atomic deformation functions describe the static deformation densities of the spherical free atoms due to aspherical valence-electron distributions. Consequently, the positional and thermal atomic parameters are expected to be free of bias introduced by bonding effects.

In the present study the B and C deformation functions were given the values $\alpha(B) = 5{\cdot}0$ and $\alpha(C) = 6{\cdot}0$. No variation of the α's was attempted throughout the refinement. The complete set of deformation functions compatible with the atomic site symmetries comprised 76 members up to hexadecapoles with 55 independently adjustable coefficients, which all started with zero values.

With the total of 69 variables the refinement was stopped at $R_w = 0{\cdot}028$. This value is considerably improved in comparison with the conventional all-data refinement. The results of the multipole expansion refinement are listed in Tables 3 to 6. Additionally, the final coefficients dominating the expansion of the deformation density $[c_{jl} > 3\sigma(c_{jl})]$ are listed in Table 7.

Table 7. *Multipole coefficients* C_{jl} *exceeding* $3{\cdot}0\sigma(c_{jl})$, $\alpha = \sqrt{2}-1$

Atom	First neighbor	Second neighbor	Multipole order N	Direction	C_{jl}
C	B(3)	B(1)	1	100	0·77
			3	110	−1·49
				1$\bar{1}$0	−1·70
B(1)	C	B(2)	2	110	0·58
			3	110	2·27
				1$\bar{1}$0	1·43
				101	1·32
				111	−1·99
				1$\bar{1}\bar{1}$	−1·70
			4	α11	0·65
				11α	−0·92
B(2)	B(1)	C	0		0·33
			1	100	−0·29
			3	110	1·49
				1$\bar{1}$0	−0·97
				011	0·56
				111	−1·41
				1$\bar{1}\bar{1}$	1·25
			4	010	0·61
				α11	−0·68
				1α1	0·45
				$\bar{\alpha}$11	1·24
				1$\bar{\alpha}$1	−0·53
B(3)	C	B(1)	4	100	4·85
				010	−1·61

Discussion of the results

The structure refinement corroborates the earlier geometric results (Clark & Hoard, 1943; Will & Kossobutzki, 1976*a*). A schematic drawing of the C–B–C chain and two adjacent B_{12} icosahedra is depicted in Fig. 2. The B_{12} unit is somewhat distorted from ideal icosahedral symmetry. As a consequence there are four distinguishable intra-icosahedral B–B bonds with lengths between 1·773 and 1·823 Å, which form the edges of three different triangles on the surface of the icosahedron. Assuming a straight reciprocal bond-length bond-strength relation, B(1)–B(1) is slightly stronger than the two different B(1)–B(2) bonds, followed by B(2)–B(2). Since the B(1) atoms are connected to C, while B(2) atoms are only involved in B–B bonds, it seems that the B–B interaction is strengthened with the number of C atoms as next B neighbors (compare also Will & Kossobutzki, 1976*b*). The mean B–B distance in the icosahedron is 1·799 Å, which is in agreement with related compounds like

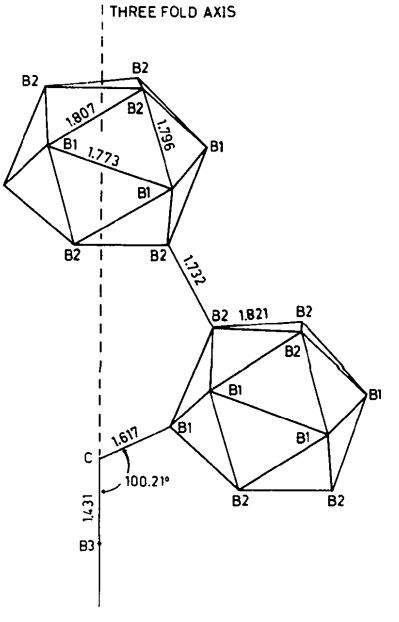

Fig. 2. Bond distances (Å) in and between the two structural units of $B_{13}C_2$.

AlB_{10} (Will, 1967), C_4AlB_{24} (Will, 1969), or β-rhombohedral boron (Hoard, Sullenger, Kennard & Hughes, 1970).

The inter-icosahedral B(2)–B(2) bond of 1·731 Å is significantly shorter than the intra-icosahedral bonds. This strongest B–B interaction found in the structure indicates that the bond mechanism between the icosahedra is different from the intra-icosahedral one.

The C atom is fourfold coordinated by three B(1) atoms, belonging to symmetry-related icosahedra, and B(3) of the C–B–C chain. The resulting B_4C configuration is considerably distorted from tetrahedral sp^3 symmetry. The three B(1) atoms and C form a flat trigonal pyramid, resulting in angles B(1)–C–B(3) 100·21 (4) and B(1)–C–B(1) 116·93 (3)°. The C–B(1) bond of 1·617 Å is larger than the known average C–B length of about 1·56 Å as found in organic compounds (*International Tables for X-ray Crystallography*, 1974; Gupta, Kirfel & Will, 1977) whereas the B(3)–C distance of 1·431 Å indicates a very strong C–B interaction comparable with a partial double bond. This deformation of the usual sp^3 hybridization of the C valence electrons turns the C–B–C chain into the strongest building unit of the structure.

The differences between the positional parameters from the various conventional refinements are small and do not lead to significant changes of the interatomic distances. Distances agreeing within the limits of error with the former values are also derived from the multipole refinement, except the B(3)–C distance, which is significantly elongated by 0·007 Å. An explanation can be found in Table 7 showing for C a significant dipole deformation function oriented along C–B(3). This implies an asymmetric C electron density distribution along c_0, which leads to a shift of the C position towards B(3), when fitting the conventional spherical-atom model to the observed density. Supporting evidence is given by the small but observable increase of the B(3)–C distance with the increase of the data cut-off angle in the high-order refinements.

The high-order data cut-off angle decreases the u_{ij} differently and the final values agree well with the corresponding values derived from the multipole refinement.

The thermal parameters and the influence of the different refinements on the atomic u_{ij} can be observed in Table 5 and from an *ORTEP* drawing (Johnson, 1965) of the asymmetric unit (Fig. 3). The vibrational behavior of B(1) is isotropic, while B(2) displays somewhat stronger vibrations perpendicular to c_0. Nevertheless, in a first approximation, the B_{12} unit represents a rigid body performing isotropic vibrations. This does not apply to the same extent for the chain atoms. The chain atoms show about twice as much vibration along c_0 and B(3) is again approximately isotropic (note the HO influence), but the vibrations of C are rather anisotropic. Perpendicular to c_0, atom C vibrates like the icosahedron due to the three bonds with B(1), while parallel to c_0 the C vibrates like B(3), to which it is strongly attached. Hence the chain can be considered as a rigid body only with respect to c_0.

A further check of the physical significance of the u_{ij} was performed by the rigid-bond test (Hirshfeld, 1976). The successful separation of vibrational smearing and charge deformation due to chemical bonding can be tested by comparison of the vibration ellipsoids of bonded atom pairs, which should have equal amplitudes $z^2_{A,B}$ and $z^2_{B,A}$ in the bond direction. The calculation of the r.m.s. discrepancy of the differences $(z^2_{A,B} - z^2_{B,A})$ for each refinement may serve as a statistical indication of the improvement of the derivation of vibrational parameters.

Table 8 shows the mutual thermal vibrations as derived from the different refinements. The r.m.s. discrepancy is dominated by the B(3)–C contribution, which decreases with increasing data cut-off angle. The final z^2 values of bonded atoms (HO2, HO3, multipole expansion) agree well within the limits of error, and hence we can conclude that the corresponding u_{ij} express atomic vibrations without significant bias by valence-electron distribution.

Table 8. *Selected mutual thermal vibrations* $z^2_{A,B}$ *and* $z^2_{B,A}$ ($\times 10^4$ Å^2)

Refinement	All data	HO1	HO2	HO3	Multipole expansion
B(1)–C	47 47	44 41	44 40	44 40	41 39
B(1)–B(2)	51 51	46 44	44 43	44 43	48 44
B(3)–C	135 171	126 134	118 123	115 118	113 117
r.m.s. discrepancy	20·8	5·0	3·7	2·9	2·8

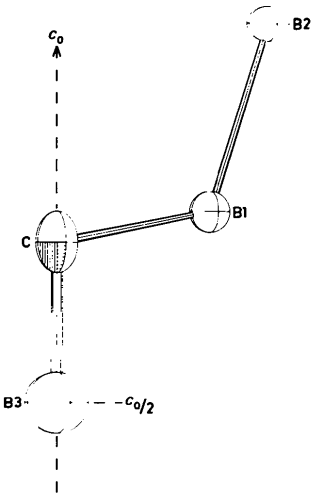

Fig. 3. *ORTEP* drawing of the asymmetric unit of $B_{13}C_2$. Thermal vibrations are exaggerated by a factor of 2·5.

First estimates of the atomic charges were derived from the least-squares adjustments of the occupancies. The scaling of the form-factor curves in the course of the refinement and taking the refined values as good approximations of the atomic charges is true only for low-angle data. For this reason an additional refinement was carried out with reflections with $s \leq 0{\cdot}65$ Å^{-1} only.

High-angle reflections contain almost only contributions of the electron distribution concentrated closely around the nuclear position. The multiplicity results of high-order refinements should therefore yield the number of electrons of the element on the position considered. Hence, these results may be regarded as a check for the stoichiometry of the sample and for disorder of the constituent atoms. In Table 9 the figures representing the number of electrons (Z) per site are listed, as derived from the five conventional refinements. For comparison we have included in the last column corresponding values calculated by spatial integration of the refined deformation function sets. The latter results, however, suffer from the fixed exponential tails on the deformation functions and hence may represent gross over- or under-estimates.

From the individual electron numbers the net charges of both structural units, the B_{12} icosahedron and the C—B—C chain, were calculated to obtain information about a possible charge transfer as demanded by the theory of Longuet-Higgins & Roberts (1955).

Table 9 shows a clear trend in the charge distribution. The low-order and all-data refinements exhibit a charge transfer within the chain from B(3) to C, giving charge estimates of about +0·5 e for B(3) and −0·25 e for C, but the chain itself remains neutral. Consequently neutrality is found for the B_{12} unit. B(1) and B(2) do not show any significant deviation from neutrality themselves. In conclusion, there is so far no experimental evidence of a charge transfer between the two structural units. Both seem to be neutral and to be held together by other than Coulomb forces. In addition to this finding one can infer from the high-order results that in the crystal under investigation there is no substitution of B(1) and/or B(2) by C, which supports the stoichiometry of the compound.

The individual charges calculated from the multipole expansion refinement represent certainly gross over-estimates, especially for B(3). They indicate that the α's describing the radial distribution of the deformation functions may not be large enough to prevent long exponential tails. Additionally, it may be useful to assign an individual α to B(3). These findings deserve further attention and we intend to study the influence of the α coefficient in more detail.

In spite of these shortcomings, the overall charge transfer, resulting from the individual charges, is close to zero again. Hence both refinement procedures reveal the same result; there is no indication that two electrons necessary for a closed shell configuration of the B_{12} icosahedron are provided by the chain atoms, at least for the compound under investigation.

Table 9. *Atomic charges Z(e) from least-squares refinements (theoretical $\sum Z = 77$)*

Refinement	LO	All data	HO1	HO2	HO3	Multipole expansion
B(1)	4·93 (4)	4·97 (2)	5·01 (1)	5·00 (1)	5·00 (2)	5·76
B(2)	5·05 (4)	5·02 (2)	5·00 (1)	5·00 (1)	5·00 (2)	4·23
B(3)	4·58 (10)	4·67 (5)	4·95 (5)	4·97 (6)	4·98 (8)	1·43
C	6·28 (7)	6·21 (3)	5·97 (3)	5·99 (3)	5·99 (4)	7·83
$\sum Z$	77·04	77·00	76·97	76·97	76·98	77·0
ΔZ_{ch}	+0·14	+0·07	−0·11	−0·05	−0·04	+0·08
ΔZ_{icos}	−0·10	−0·07	+0·08	0·0	+0·02	−0·08

Conclusion

The conventional all-data refinements on the experimental data of $B_{13}C_2$ have shown that the spherical free-atom model leads to positional and thermal parameters, some of which are considerably biased by bonding effects. The subsequent high-order refinements and the multipole expansion refinement yielded improved R values and comparable parameters of physical significance. This is especially true for the thermal parameters and for the scale factor and it supports the need for high-order refinement techniques. The scale factors display a clear trend (Table 3) with respect to the adequacy of the employed electron density model. The values obtained from the HO refinements and the multipole expansion refinement agree within the limits of error. The latter ($K = 0{\cdot}453$) is close to the weighted average and hence may be regarded as the best value to be used for subsequent calculations.

Both structural units can be regarded as neutral. A charge redistribution within the B_{12} icosahedron is not detectable.

For the C—B—C chain all results indicate a considerable deviation from the spherical valence density distribution.

Such deviations due to bonding can be studied by syntheses of valence and dynamic deformation density maps based on the bias-free atomic parameters. Static deformation-density distributions can be calculated from the refined coefficients of the localized linear combinations of deformation functions. Subsequent investigations of this kind are in progress and the results will be reported in the continuing parts of this work.

This work has received the support of the Deutsche Forschungsgemeinschaft, which is gratefully acknowledged. We also thank Professor Amberger, Munich, for providing the crystal.

References

AMBERGER, E. (1977). Private communication.
AMBERGER, E., DRUMINSKI, M. & PLOOG, K. (1971). *J. Less-Common Met.* **23**, 43–52.
BUSING, W. R., MARTIN, K. O. & LEVY, H. A. (1962). *ORFLS*. Report ORNL-TM-305. Oak Ridge National Laboratory, Tennessee.
CLARK, K. H. & HOARD, J. L. (1943). *J. Am. Chem. Soc.* **65**, 2115–2119.
GUPTA, A., KIRFEL, A. & WILL, G. (1977). *Acta Cryst.* B**33**, 637–641.
HAREL, M. & HIRSHFELD, F. L. (1975). *Acta Cryst.* B**31**, 162–172.
HIRSHFELD, F. L. (1971). *Acta Cryst.* B**27**, 769–781.
HIRSHFELD, F. L. (1976). *Acta Cryst.* A**32**, 239–244.
HOARD, J. L., SULLENGER, D. B., KENNARD, C. H. & HUGHES, R. E. (1970). *J. Solid State Chem.* **1**, 268–277.
International Tables for X-ray Crystallography (1974). Vol. IV. Birmingham: Kynoch Press.
JOHNSON, C. K. (1965). *ORTEP*. Report ORNL-3794. Oak Ridge National Laboratory, Tennessee.
LONGUET-HIGGINS, H. C. & ROBERTS, M. DE V. (1955). *Proc. R. Soc. London, Ser. A*, **230**, 110–119.
MATKOVICH, V. I. & ECONOMY, J. (1977). *Boron and Refractory Borides*, pp. 98–114. Berlin: Springer-Verlag.
WILL, G. (1967). *Acta Cryst.* **23**, 1071–1079.
WILL, G. (1969). *Acta Cryst.* B**25**, 1219–1222.
WILL, G. & KOSSOBUTZKI, K. H. (1976*a*). *J. Less-Common Met.* **44**, 87–97.
WILL, G. & KOSSOBUTZKI, K. H. (1976*b*). *J. Less-Common Met.* **47**, 43–48.
ZACHARIASEN, W. H. (1963). *Acta Cryst.* **16**, 1139–1144.

Acta Cryst. (1979). B**35**, 1059–1062

Refinement of the Sr_2EuFeO_5 and Sr_2EuAlO_5 Structures

BY M. DROFENIK* AND L. GOLIČ

Institute 'Jožef Stefan', Chemistry Department, University of Ljubljana, 61000 Ljubljana, Yugoslavia

(*Received* 8 *November* 1978; *accepted* 7 *February* 1979)

Abstract

Crystals of Sr_2EuFeO_5 and Sr_2EuAlO_5 are tetragonal, space group $I4/mcm$ and $Z = 4$. Cell parameters for Sr_2EuFeO_5 are $a = 6{\cdot}812\ (3)$, $c = 11{\cdot}263\ (3)$ Å, and for Sr_2EuAlO_5 $a = 6{\cdot}742\ (1)$, $c = 10{\cdot}970\ (1)$ Å. The two compounds are isostructural with Cs_3CoCl_5. The structures were refined to final R values of 0·021 and 0·022 respectively. The structures contain FeO_4 or AlO_4 tetrahedra. The Sr and Eu atoms are statistically distributed over one position, 8(*h*). The O atom which is not a part of the tetrahedron is octahedrally coordinated by Sr and Eu.

Introduction

In our study of the ternary system $SrO–Eu_2O_3–Fe_2O_3$ (Drofenik, Kolar & Golič, 1974*a*) we reported the occurrence of the ternary phase Sr_2EuFeO_5. Monocrystals of the compounds Sr_2EuFeO_5 and Sr_2EuAlO_5 have been grown (Drofenik, Kolar & Golič, 1974*b*, 1979) and the structure model has been proposed. The present work describes the refinement of this structure.

This group of compounds belongs to a group of alkaline-earth pentaoxometallates, with strontium substituted by a rare-earth atom.

During his extensive work Scholder (1958) prepared a series of isotypic compounds with the general formula Ba_3MO_5 (M = Ti, V, Cr, Mn, Fe, Co, Si, Ge). Later, Gotsmann (1962) and Letzelter (1960) prepared some ternary compounds Sr_2LaAlO_5 and Ba_2LaMO_5 (M = Mn, Fe, Co, Al, Ga).

During their study of silicates, Dent Glasser & Glasser (1965), and Dent Glasser (1965) solved the structure of Sr_3SiO_5 and described the structural relationship between Sr_3SiO_5, Cd_3SiO_5 and Ca_3SiO_5. Mansmann (1965) found that three barium pentaoxometallates Ba_3MO_5 were isotypic with Cs_3CoCl_5 (Powell & Wells, 1935), and reported that the structure of Sr_3SiO_5 ($P4/ncc$) is isotypic with Cs_3CoCl_5 ($I4/mcm$) up to the second non-metal position, which causes the transition from a centrosymmetric to a primitive lattice. Also Eysel (1970) has reported the structures of two pentafluoroberyllates, K_3BeF_5 and Rb_3BeF_5, which are isotypic with Cs_3CoCl_5, and reviewed this group of compounds.

* To whom correspondence should be addressed.

0567-7408/79/051059-04$01.00